

Multi-objective optimization of reactive extrusion by genetic algorithms

Guofang Zhang,¹ Min Zhang,² Yuxi Jia¹

¹School of Materials Science & Engineering, Shandong University, Jinan 250061, People's Republic of China

²School of Mechanical Engineering, Shandong University, Jinan 250061, People's Republic of China

Correspondence to: Y. Jia (E-mail: jia_yuxi@sdu.edu.cn)

ABSTRACT: In reactive extrusion processes for polymerization, a multi-objective optimization model maximizing the monomer conversion whilst ensuring the low energy consumption was constructed. The selections of reactive processing conditions could be set automatically using an optimization methodology based on genetic algorithms coupled with the numerical simulation routines. Various case studies were discussed. Comparison with experimental data indicates that the design of processing conditions can be performed according to the prespecified objectives. © 2014 Wiley Periodicals, Inc. *J. Appl. Polym. Sci.* **2015**, *132*, 41862.

KEYWORDS: extrusion; radical polymerization; synthesis and processing; theory and modeling

Received 15 August 2014; accepted 30 November 2014

DOI: 10.1002/app.41862

INTRODUCTION

Reactive extrusion involves the synthesis or modification of polymers by melt-phase reactions in twin-screw extruders.^{1,2} The chemical reactions involve bulk polymerization, grafting, blending, crosslinking and degradation of polymers. The high viscosities, high temperatures, and short residence times make it difficult to design and to control a chemical reaction. One has to deal with considerable coupling variables involved in such phenomena as fluid flow, heat transfer, and chemical reaction.³ The selections of reactive processing conditions such as the material composition, screw geometry, and operating parameters often involve a trial-and-error procedure which is very time-consuming and expensive.

One of the effective methods of solving the above problems is to establish an optimization methodology, by means of which the optimum values of processing conditions can be obtained. Because both the objective function and the constraints are nonlinear, it is difficult to build the explicit functions to directly obtain the processing parameters. Numerical simulations have been devoted to dealing with the nonlinear model equations.^{4–8} Using an implicit iterative algorithm, evolutions of key variables such as residence time, monomer conversion, average molecular weight, and fluid viscosity can be quantitatively predicted. Recently, the numerical modeling routines have been coupled to optimization methods such as the genetic algorithm and artificial neural network to set automatically the processing conditions. Using neural network method, Nascimento *et al.* proposed an optimization procedure taking into account the safe operation conditions, wear and tear of the equipment, product quality and

energy consumption, and applied the optimization approach to the industrial process of nylon-6,6 polymerization in a twin-screw extruder.^{9–11} Coupling a multi-objective evolutionary algorithm with the Ludovic software, Gaspar-Cunha *et al.* maximized the output and ensured the maximum melt temperature stays within a prescribed range in the reactive extrusion process for ϵ -caprolactone polymerization.^{12,13}

The above optimization methodology is powerful, however, it is seldom used in industrial practice for the high price and low efficiency of most existing computational tools. Most simulations were based on a one-dimensional (1D) model. The objective functions have a uniform distribution in any axial cross section of the extruder, which are different from the real conditions.⁴ Objective functions based on three-dimensional (3D) model meet well with practice, but they are always confined to the partial process.^{14,15}

The optimization methodology for reactive extrusion processes is still in its infancy and further researches should be performed. In our previous studies, we have built a 2D axisymmetrical model, introduced a semi-implicit iterative algorithm and conducted the numerical simulation of reactive extrusion processes for polymerization.¹⁶ In this article, the reactive extrusion process for the free radical bulk polymerization was chosen as the optimization system. The multi-objective optimization model taking into account the monomer conversion and the energy consumption was constructed, and then the optimization methodology based on genetic algorithms coupled with the numerical simulation routines was established. Finally, an example was studied to validate the methodology.

CONSTRUCTION OF OPTIMIZATION MODELS

Optimization Model of Monomer Conversion

For a first-order free radical polymerization initiated by initiators, the general formulation of the reaction kinetics is as follows:¹⁶

$$\frac{\partial X}{\partial t} = Ae^{-E/(RT)} c_{\text{ini}}^{1/2} (1-X) \quad (1)$$

where X denotes the monomer conversion, t the reaction time, A the apparent frequency factor, E the apparent activation energy, R the general gas constant, T the reactant temperature, and c_{ini} the initiator concentration.

Considering the short residence time in an extruder and the need of reducing monomer emission, the aim is to find operating conditions that maximize the monomer conversion

$$\max X = \max \left[1 - e^{-A c_{\text{ini}}^{1/2} t e^{-E/(RT)}} \right] \quad (2)$$

where “max”, as the same is hereinafter defined, denotes the abbreviation for “maximum”.

Optimization Model of Energy Consumption

Neglecting the power consumption associated with material mixing, radiation and conduction, the theoretical energy consumption W required by an extruder can be expressed as¹⁷

$$W = [c_p Q(T - T_{\text{in}}) + Q\Delta P/\rho] t \quad (3)$$

where c_p denotes the specific heat capacity at constant pressure, Q the mass flow rate, T_{in} the material temperature at the inlet of the extruder, ΔP the discharge pressure, and ρ the material density.

The material temperature, mass flow rate, discharge pressure, and reaction time are expected to be as low as possible in terms of energy-conservation, which may result in low monomer conversion. To solve this conflict, maximization of the monomer conversion per unit energy consumption is introduced as an objective function

$$\max \frac{X}{W} = \max \frac{1 - e^{-A c_{\text{ini}}^{1/2} t e^{-E/(RT)}}}{[Q c_p (T - T_{\text{in}}) + Q\Delta P/\rho] t} \quad (4)$$

Multi-Objective Optimization Model

Generally, the operating conditions that result in the minimum energy consumption per unit monomer conversion may not yield the maximum monomer conversion. It is necessary to harmonize these conflicting objectives.^{13,18,19}

The weighting coefficient method is introduced here. The two objectives, $\max X$ and $\max (X/W)$, are endowed with the different weighting coefficients ω_1 and ω_2 , respectively. So the multi-objective optimization model can be obtained

$$\max u = \max \left(\omega_1 \frac{X}{C_1} + \omega_2 \frac{C_2 X}{W} \right) \quad (5)$$

where u , as the same is hereinafter defined, denotes the multi-objective function. C_1 and C_2 denote the constants for normalization processing.¹⁸ The importance of each single objective can be considered as the criterion for setting the values of ω_1 and ω_2 .

CONSTRUCTION OF CHEMORHEOLOGICAL MODELS

The power-law constitutive equation is generally adopted to predict the shear rate dependence of the viscosity in bulk polymerization^{2,16}

$$\eta = \frac{\eta_0}{(1 + b\dot{\gamma})^c} \quad (6)$$

where η denotes the apparent viscosity and $\dot{\gamma}$ the shear rate. b and c are two parameters. The zero shear viscosity η_0 can be empirically described as a function of temperature and molecular weight^{2,16}

$$\eta_0 = \begin{cases} K_1 e^{\frac{E_\eta}{RT}} c_M \bar{M}_w & \bar{M}_{\text{eqw}} \leq M_c \\ K_2 e^{\frac{E_\eta}{RT}} c_M^{5.4} \bar{M}_w^{3.4} & \bar{M}_{\text{eqw}} > M_c \end{cases} \quad (7)$$

where E_η is the activation energy for fluid flow, c_M the mass concentration of polymer chains, \bar{M}_w the average molecular weight of polymer chains, M_c the critical molecular weight for entanglement effects in viscosity, K_1 and K_2 the material constants. The relationship between the equivalent average molecular weight \bar{M}_{eqw} and the conversion is expressed as follows:¹⁶

$$\bar{M}_{\text{eqw}} = \bar{M}_w X + M_m (1 - X) \quad (8)$$

where M_m is the molecular weight of the monomer.

OPTIMIZATION METHODOLOGY

As shown in Figure 1, the genetic algorithm was used to optimize the processing conditions, and the finite volume simulation of reactive extrusion processes was applied to solve the multi-objective functions. The specific steps are shown as follows:

1. Population initialization: Define G as the number of evolutionary generations and set the initial and maximum numbers of generations to be zero and G_{max} , respectively. Then the initial generation is generated randomly, taking into account the parameters to optimize and the corresponding limits of variation.

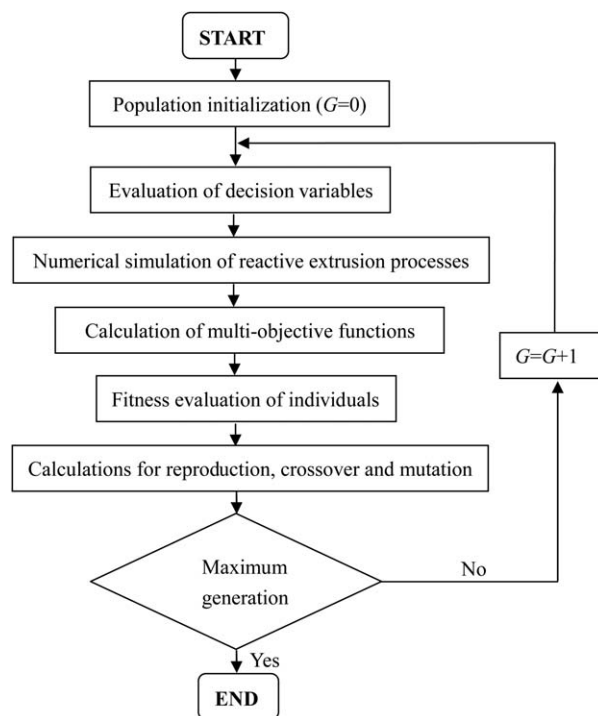


Figure 1. Flow chart of optimization methodology.

Table I. Parameters of the Extruder and Material Properties^{2,16}

Parameters	Numerical values
Nominal diameter of screws D	50 mm
Centerline distance of screws	45 mm
Slenderness ratio of screws L/D	14
Number of thread starts	2
Lead of screws	52 mm
Density of the material ρ	$0.878 \times 10^3 \text{ kg m}^{-3}$
Specific heat capacity at constant pressure c_p	$2.01 \times 10^3 \text{ J kg}^{-1} \text{ K}^{-1}$
Molecular weight of monomer M_m	142 g mol^{-1}
Initial concentration of monomer	$6183.1 \text{ mol m}^{-3}$
Initial concentration of initiator	70.0 mol m^{-3}
Apparent frequency factor A	$7.67 \times 10^8 \text{ m}^{3/2} \text{ mol}^{-1/2} \text{ s}^{-1}$
Apparent activation energy E	$9.20 \times 10^4 \text{ J mol}^{-1}$
The parameter b in power-law equation	0.2649 s
The parameter c in power-law equation	0.7899
Critical molecular weight for entanglement effects M_c	30000 g mol^{-1}
Activation energy for fluid flow E_η	$1.76 \times 10^5 \text{ J mol}^{-1}$
Mass flow rate Q	50 g mol^{-1}

- Evaluation of decision variables: The numerical value of each individual in the population of decision variables is obtained by decoding each individual in the current population.
- Numerical simulation: For each individual in the population of decision variables, the finite volume analysis of reactive extrusion processes is performed to get the values of the objective functions by means of a semi-implicit iterative algorithm. Detailed descriptions of the numerical algorithm have been reported in Ref. [16].
- Fitness evaluation: The fitness of each individual in the population of decision variables is calculated and ranked to determine the selection rate.
- Calculations for reproduction, crossover, and mutation: A new generation is produced by means of the selection rate, crossover rate, and mutation rate.
- Termination judgement: The current number of the generation is added one, namely $G+1 \rightarrow G$, and then the procedure in Step 2 through Step 5 is repeated until the serial number of the generation reaches the maximum number of generations.

EXAMPLES AND VERIFICATION

Case Studies

To validate the rationality of the constructed models, the multi-objective optimization of the reactive extrusion process for

n-butylmethacrylate (*n*-BMA) polymerization was investigated, and the simulated results were compared with Jongbloed's experimental data.²⁰ The parameters of the extruder and material properties are shown in Table I^{16,20} and the input data for optimization are listed in Table II.

It can be seen from Eqs. (2) and (4) that the objective functions are mainly influenced by the barrel temperature, the mass flow rate, the discharge pressure, the reaction time, and the initiator concentration. The discharge pressure was measured with a pressure transducer in the die region. Experimental results from Ref. [20] showed that the discharge pressure was about 10^5 Pa. The required heat energy was three orders of magnitude higher than the required mechanical energy, which indicates that the second term in the right section of Eq. (3) can be neglected.

In the simulation, the space of fluid flow was equivalently considered as a long axisymmetrical space and the inlet velocity of the reactor model is calculated by the mass flow rate.¹⁶ The reaction time can be calculated by

$$\Delta t(I, J) = \frac{\Delta l}{v(I, J)} \quad (9)$$

where $\Delta t(I, J)$ denotes the time step on the J^{th} space point in the I^{th} time step, Δl the distance between two adjacent nodes, and $v(I, J)$ the axial component of the flow velocity on the J^{th} space point in the I^{th} time step. The experiment was limited to $14D$ by insertion of a seal although the maximum screw length L is $25D$, where D denotes the screw diameter. So the screw length can be treated as an adjusted parameter in this study.

The extruder has five heating zones. The last four zones were kept at a uniform temperature T_{2-5} , whilst the first zone, closest to the feed port, was kept at another lower temperature T_1 .

As mentioned above, four case studies will be analyzed separately. Dealing exclusively with the barrel temperature T_b ($L=14D$, $Q=50 \text{ g min}^{-1}$), the first three cases are used to compare with experimental data and determine the weighting coefficients ω_1 and ω_2

$$\text{Case 1: } \max u(T_b) = \max \left(\omega_1 \frac{X}{C_1} + \omega_2 \frac{C_2 X}{W} \right) \quad \omega_1=0, \omega_2=1$$

$$\text{Case 2: } \max u(T_b) = \max \left(\omega_1 \frac{X}{C_1} + \omega_2 \frac{C_2 X}{W} \right) \quad \omega_1=1, \omega_2=0$$

$$\text{Case 3: } \max u(T_b) = \max \left(\omega_1 \frac{X}{C_1} + \omega_2 \frac{C_2 X}{W} \right) \quad \omega_1=0.8, \omega_2=0.2$$

The fourth case optimizes simultaneously the barrel temperature and the screw length

$$\text{Case 4: } \max u(T_b, L) = \max \left(\omega_1 \frac{X}{C_1} + \omega_2 \frac{C_2 X}{W} \right) \quad \omega_1=0.8, \omega_2=0.2$$

According to the homopolymerization of BMA and the copolymerization of BMA with HBMA, the constraints of

Table II. Main Input Data for the Optimization System

Parameters	Numerical values
Population size	5
Maximum number of generations G_{\max}	200
Crossover rate	0.5
Mutation rate	0.02

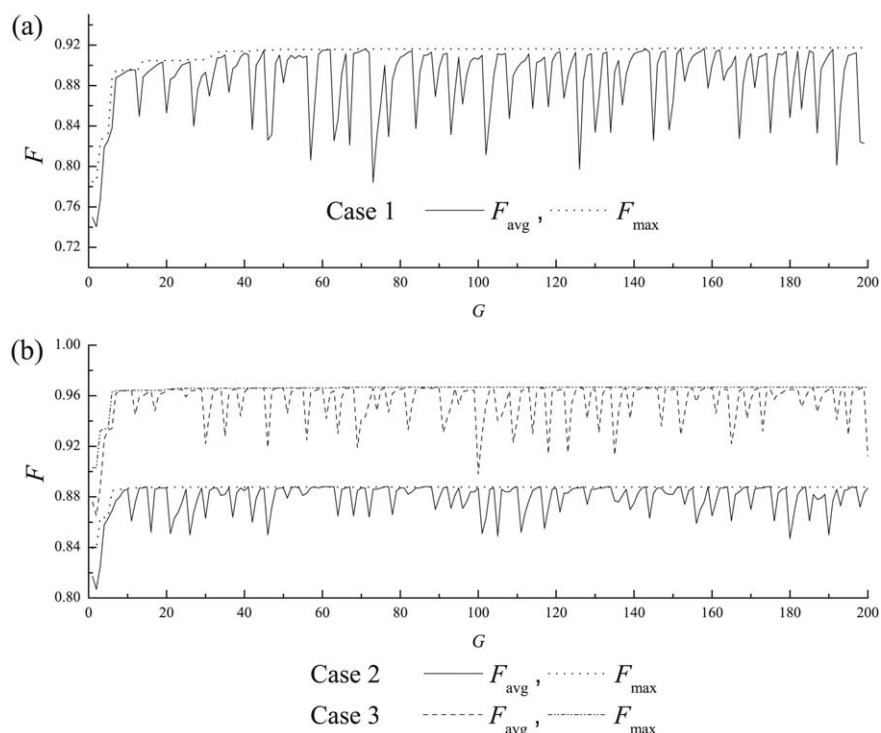


Figure 2. Evolution of the average fitness and maximum fitness of each population (a) Case 1; (b) Cases 2 and 3.

the barrel temperatures are $100^{\circ}\text{C} \leq T_1 \leq 120^{\circ}\text{C}$ and $130^{\circ}\text{C} \leq T_{2-5} \leq 150^{\circ}\text{C}$. According to the requirements of energy saving and emission reducing, the constraint of the screw length is $13 \leq L/D \leq 15$ ($D=0.05\text{m}$).

The fitness of each individual in the population F is defined as the absolute value of the multi-objective function

$$F(T_b, L) = |u(T_b, L)| \quad (10)$$

Optimization of Barrel Temperature

As shown in Figure 2, the average population fitness F_{avg} increases in the initial evolution process and then varies with the increase of evolution generations, and the maximum population fitness F_{max} gets to a steady state when it evolves to gen-

eration 50 for Case 1 and generation 20 for Cases 2 and 3. This phenomenon indicates that the numerical values of the decision variables corresponding to the maximum fitness in each population are preserved for the next population and that the optimal objective has been obtained.

Figure 3 shows the evolutions of the barrel temperature corresponding to the maximum fitness in each population. The optimum barrel temperatures for Cases 1–3 are $T_1=100^{\circ}\text{C}$ and $T_{2-5}=130^{\circ}\text{C}$, $T_1=120^{\circ}\text{C}$ and $T_{2-5}=135^{\circ}\text{C}$, $T_1=100^{\circ}\text{C}$ and $T_{2-5}=133^{\circ}\text{C}$, respectively.

Verification

Taking the optimum barrel temperature as operating conditions, the numerical simulation of the reactive extrusion is performed

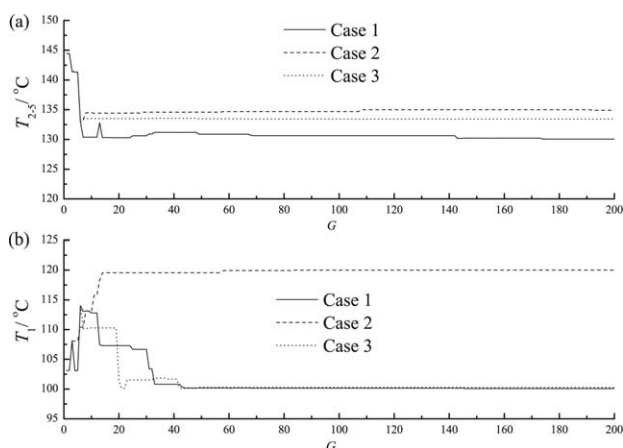


Figure 3. Evolution of the barrel temperature corresponding to the maximum fitness of each population (a) T_{2-5} ; (b) T_1 .

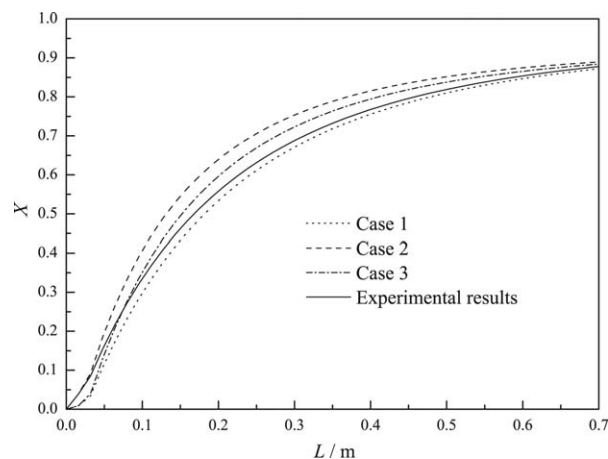


Figure 4. Evolution of monomer conversion along the axial direction of the extruder.

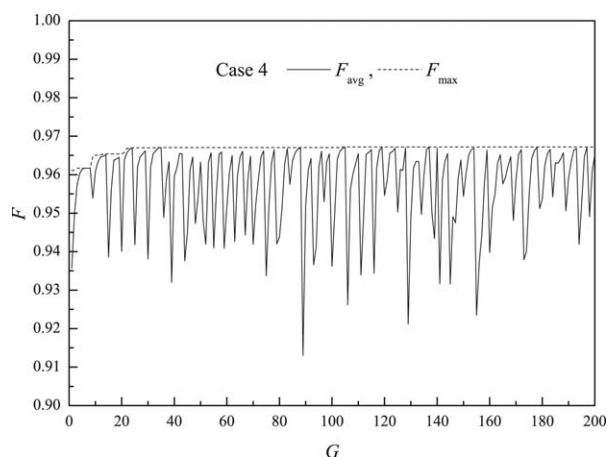


Figure 5. Evolution of the average fitness and maximum fitness of each population in Case 4.

using the semi-implicit iterative algorithm. The evolution of the monomer conversion along the axial direction of the extruder is shown in Figure 4. It can be seen that the simulated results meet well with the experimental results ($L = 14D$, $Q = 50 \text{ g min}^{-1}$, $T_1 = 120^\circ\text{C}$, $T_{2-5} = 130^\circ\text{C}$).

The monomer conversions for Cases 1–3 and the experiment are 87.8%, 88.9%, 88.4%, and 87.8%, respectively. The energy consumptions per unit conversion for Cases 1–3 and the experiment are 91.12, 97.28, 91.39, and 95.00 kJ, respectively. It can be seen that the minimum monomer conversion and energy consumption per unit conversion are gained in Case 1, the maximum ones are obtained in Case 2, and the values in Case 3 falls between the ones in Cases 1 and 2. The result indicates that the multi-objective optimization model can meet the pre-specified objectives by setting the values of ω_1 and ω_2 .

Case 1 meets well with the experimental data. However, considering the short residence time in an extruder and the need of reducing monomer emission, the high monomer conversion is always put as the first consideration, and then is the low energy consumption. Therefore, Case 3 meets well with industrial practice. The values of ω_1 and ω_2 are set to 0.8 and 0.2, respectively, in the following optimization.

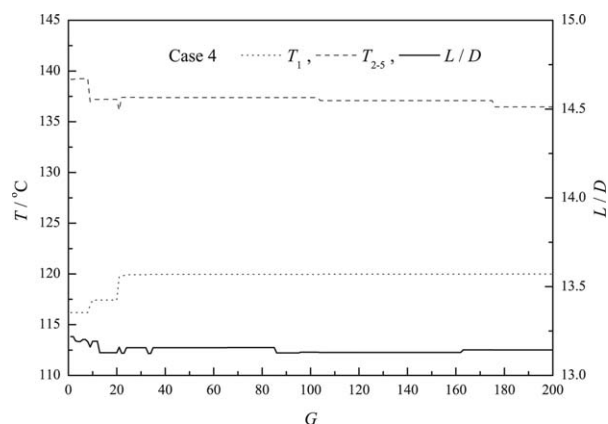


Figure 6. Evolution of the barrel temperature and screw length corresponding to the maximum fitness of each population in Case 4.

Optimization of Barrel Temperature and Screw Length

The evolutions of the average population fitness and the maximum population fitness of Case 4 are shown in Figure 5. It can be seen that the maximum population fitness gets to a steady state when it evolves to generation 40, indicating that the optimal objective has been obtained.

Figure 6 shows the evolutions of the barrel temperature and screw length corresponding to the maximum fitness in each population. The optimum values of the decision variables are $T_1 = 120^\circ\text{C}$, $T_{2-5} = 136^\circ\text{C}$, $L/D = 13$.

CONCLUSIONS

1. A multi-objective optimization model of reactive extrusion process for polymerization was constructed to maximize the monomer conversion whilst ensure the low energy consumption.
2. The optimization methodology for reactive extrusion processes was established, in which the genetic algorithm was used to optimize the processing conditions, and the finite volume simulation was applied to solve the multi-objective functions.
3. Comparison with experimental data validates the rationality of the constructed models and the optimization methodology. The processing conditions can be designed according to the pre-specified objectives.

ACKNOWLEDGMENTS

This work was supported by the National Natural Science Foundation of China (51103080) and the China Postdoctoral Science Foundation (20110491563).

REFERENCES

1. Moad, G. *Prog. Polym. Sci.* **1999**, *24*, 81.
2. Cassagnau, P.; Bounor-Legare, V.; Fenouillot, F. *Int. Polym. Proc.* **2007**, *22*, 218.
3. Janssen, L. P. B. M. *Polym. Eng. Sci.* **2010**, *38*, 2010.
4. Zhu, L.; Narh, K. A.; Hyun, K. S. *Adv. Polym. Technol.* **2005**, *24*, 183.
5. Vergnes, B. and Berzin, F. C. R. *Chim.* **2006**, *9*, 1409.
6. Banu, I.; Puaux, J. P.; Bozga, G.; Nagy, I. *Macromol. Symp.* **2010**, *289*, 108.
7. Garge, S. C.; Wetzel, M. D.; Ogunnaike, B. A. *J. Proc. Contr.* **2012**, *22*, 1457.
8. Ortiz-Rodriguez, E.; Tzoganakis, C. *Int. Polym. Proc.* **2012**, *27*, 442.
9. Nascimento, C. A. O.; Giudici, R. *Comput. Chem. Eng.* **1998**, *22*, 595.
10. Nascimento, C. A. O.; Giudici, R.; Scherbakoff, N. *J. Appl. Polym. Sci.* **1999**, *72*, 905.
11. Nascimento, C. A. O.; Giudici, R.; Guardani, R. *Comput. Chem. Eng.* **2000**, *24*, 2303.
12. Gaspar-Cunha, A.; Poulesquen, A.; Vergnes, B.; Covas, J. A. *Int. Polym. Proc.* **2002**, *17*, 201.

13. Gaspar-Cunha, A.; Covas, J. A.; Vergnes, B. *Polym. Eng. Sci.* **2005**, *45*, 1159.
14. Strutt, D.; Tzoganakis, C.; Duever, T. A. *Adv. Polym. Technol.* **2000**, *19*, 22.
15. Zhu, L.; Narh, K. A.; Hyun, K. S. *Int. J. Heat Mass Transf.* **2005**, *48*, 3411.
16. Jia, Y. X.; Zhang, G. F.; Wu, L. L.; Sun, S.; Zhao, G. Q.; An, L. J. *Polym. Eng. Sci.* **2007**, *47*, 667.
17. Liang, M.; Huff, H. E.; Hsieh, F. H. *J. Food Sci.* **2002**, *67*, 1803.
18. Jia, Y. X.; Sun, S.; Liu, L. L.; Mu, Y.; An, L. J. *Acta Mater.* **2004**, *52*, 4153.
19. Bhaskar, V.; Gupta, S. K.; Ray, A. K. *Comput. Chem. Eng.* **2001**, *25*, 391.
20. Jongbloed, H. A.; Kiewiet, J. A.; Van Dijk, J. H.; Janssen, L. P. B. M. *Polym. Eng. Sci.* **1995**, *35*, 1569.